Computational Spectroscopy Using MULTIMODE and Machine-Learned Potentials in Python Too

Chen Qu,[1] Thomas C. Allison,[2] Paul L. Houston,[3] Riccardo Conte,[4] Apurba Nandi,[5] and Joel M. Bowman[6]

[1])*Independent Researcher, Toronto, Ontario M9B 0E3, Canada*

[2])*National Institute of Standards and Technology, 100 Bureau Drive, Gaithersburg, MD 20899, USA*

[3])*Department of Chemistry and Chemical Biology, Cornell University, Ithaca, New York 14853, U.S.A.*

[4])*Dipartimento di Chimica, Università degli Studi di Milano, via Golgi 19, 20133 Milano, Italy*

[5])*Department of Physics and Materials Science, University of Luxembourg, L-1511, Luxembourg City, Luxembourg*

[6])*Department of Chemistry and Cherry L. Emerson Center for Scientific Computation, Emory University, Atlanta, Georgia 30322, U.S.A.*

(*Electronic mail: jmbowma@emory.edu)

(*Electronic mail: szquchen@gmail.com)

(Dated: 5 January 2026)

Computational vibrational spectroscopy beyond the harmonic approximation relies on the molecular potential and ideally dipole and possibly higher moments of charge distributions. In the past decade there has been a paradigm shift in generating highly accurate Machine-Learned potentials (MLPs). These are precise fits to thousands of electronic energies, using modern methods of regression. With such MLPs it is possible to combine these with the variety of post-harmonic quantum methods ranging from perturbation theory to full variational calculations. After a short review of these methods, we focus on vibrational self-consistent field and configuration interaction (VSCF/VCI) calculations, as implemented in the code MULTIMODE. Two applications of this software to challenging parts of infrared spectra of the formic acid dimer and the protonated oxalate anion are presented. Two new interfaces to MULTIMODE are then given. One is a python-based GUI to enable user-friendly input to MULTIMODE. The second, PyFort, is an interface, which is written in Fortran, to use MLPs written in Python in MULTIMODE via a C wrapper. Demonstrations of this are given for a PhysNet potential of Meuwly and co-workers for protonated oxalate anion ($C_2O_4H^-$) and for the "universal" force field MACE-OFF of Csányi and co-workers. MULTIMODE VSCF/VCI vibrational energies of $C_2O_4H^-$ using the PhysNet MLP agree well with those using a permutationally invariant potential, trained on the datasets used to train the PhysNet MLP. A test of the MACE-OFF interface is done for H_2CO. The PyFort software for both these examples is provided in Supplementary Material.

I. INTRODUCTION

Computational infrared (IR) spectroscopy, of molecules, molecular clusters, etc. is a large, active area of computational spectroscopy. Computational approaches include classical, semi-classical, and quantum ones. Within these broad categories there are numerous variations; many are reviewed in the book "Vibrational Dynamics of Molecules".[1] Earlier reviews, special journal issues, and perspectives devoted to this topic are available for in-depth study.[2–7].

Computational approaches to IR spectroscopy, ranging from the most approximate uncoupled double harmonic oscillator model (harmonic wavefunctions and linear dipole moment) to full vibrational configuration interaction (VCI) approach (which is exact, in principle), provide the critical assignment and interpretation of the spectral bands. While the double harmonic approach provides the simplest interpretation, it does not apply to combination and overtone bands, etc. The rigorous VCI approach with an accurate dipole moment surface can describe these bands and also complex experimental bands. Although not the focus of this article, the first post-harmonic approach developed historically is second order perturbation theory (VPT2).[8]. This approach and generalizations to it to deal with Fermi and other resonances have become one of the major workhorses in the field.[9–19] The method requires at least a partial fourth-order force field, and we will return to this below.

VPT2 and generalized versions can fail for highly coupled or even extremely anharmonic, e.g., double-well, systems. These are of particular interest to us and are the main subject of this paper. For these challenging cases, the most widely used and successful approaches are based on VCI. The vibrational self-consistent field (VSCF) was introduced in 1978 and further developed in later years.[20–26] This method, like Hartree-Fock theory in electronic structure theory, does not describe correlation. So, analogous to work in that field, the MP2 version of it was subsequently proposed and for many years referred to as a "correlation corrected VSCF".[27,28] Configuration interaction in the virtual space of excitation of the ground state VSCF Hamiltonian was also proposed[29]. More recently, vibrational coupled cluster (VCC) theory was developed.[30,31] VCI approaches are currently widely used with many variations in the choice of coordinates, basis functions and excitation space.[2,6,32–37] General software based on VCI is also available; examples include MULTIMODE,[38–40] GENIUSH,[41,42] TROVE,[5,43] DYNAMOL,[44] PyVCI (limited to force

fields up to 6th order)[45], a VSCF/VCI module in Molpro* written by Rauhut and co-workers, using direct n-mode representations of the potential energy surface (PES),[46] and MIDAS,[47] a general code featuring VSCF, VCI, VMP2, and VCC also using direct n-mode representations of the potential.

There have also been new developments in "exact" vibrational methods, including vibrational density-matrix renormalization group (vDMRG)[48] and tree tensor network states (TTNS),[49] which is a close relative to the earlier and powerful MCTDH method.[50,51]

The form of the PES is an important aspect of the computational method used in VCI, MCTDH, vDRMG, and TTNS methods. In VPT2, the full or partial quartic force field is generally the form used. Higher-order force fields are also used in some VCI codes[45] and in numerous innovative VCI calculations, see for example, refs. 35,36,52. Recall that these force-fields are sums of products of powers of coordinates, e.g., normal coordinates are used in VPT2, the PyVCI code, and also in numerous VCI applications. The sum-of-product form is used in MCTDH; this form has been developed significantly so that it can describe large amplitude motion. The n-mode representation of the potential, described below, is yet another form of the potential that is used in MULTIMODE and other VCI codes.[53] In the current age of general machine-learned potentials (MLPs), which is highlighted here, it should be clear that an MLP can be transformed to all of these representations.

MULTIMODE is open-source computational spectroscopy software, written in Fortran, that produces vibrational and ro-vibrational energies and spectra using general MLPs. The code performs quantum mechanical calculations using the VSCF/VCI methodology for IR spectra of molecules, molecular clusters, solids, and liquids. Several strategies are available to deal with the exponential growth of the size of the Hamiltonian matrix and the quadrature space. We describe some of these below and show that they have enabled the software to be applied to molecules with 10 or more atoms, albeit with some compromises, as noted. The IR spectra of these larger systems are typically reported in the field as "vibrational only".[54] However, we note that MULTIMODE can provide line-list ro-vibrational spectra, as demonstrated for H_2CS, H_2CO,[55] and C_2H_4.[56]

Here we report new software to enhance the usability and applicability of MULTIMODE. Before doing that, as a reminder of the capability of MULTIMODE, we present IR spectra for the diffuse bands in the formic acid dimer and the protonated oxalate anion, preceded by a short re-

---

*Certain commercial equipment, instruments, or materials (or suppliers, or software, ...) are identified in this paper to foster understanding. Such identification does not imply recommendation or endorsement by the National Institute of Standards and Technology, nor does it imply that the materials or equipment identified are necessarily the best available for the purpose.

4

view of the Watson Hamiltonian and the n-mode representation of the PES. Hereafter, we use PES and MLP interchangeably.

The paper is organized as follows. First, we recall the foundational Watson Hamiltonian. This is followed by a brief review of configuration interaction and how it can be used effectively with this Hamiltonian using general machine-learned potentials for moderate and relatively large molecules. Then two challenging case studies are presented, the 10-atom formic acid dimer and the 7-atom protonated oxalate anion. The new software to enhance the usability and applicability of MULTIMODE is described. The first is a graphical user interface (GUI) written in Python to simplify the input to MULTIMODE. The second is a general interface that enables Fortran-based MULTIMODE to communicate with MLPs written in Python. Demonstrations of this interface, which we term PyFort, are made for a PhysNet potential for protonated oxalate[57] and for MACE-OFF,[58] a "universal" machine-learned force field for organic molecules.

II.   THE WATSON HAMILTONIAN

The Watson Hamiltonian (for non-linear molecules and minus the constant "Watson term") is given by[59]

$$\hat{H} = \frac{1}{2}\sum_{\alpha\beta}(\hat{J}_\alpha - \hat{\pi}_\alpha)\mu_{\alpha\beta}(\hat{J}_\beta - \hat{\pi}_\beta) - \frac{1}{2}\sum_k^F \frac{\partial^2}{\partial Q_k^2} + V(\boldsymbol{Q}), \tag{1}$$

where $\boldsymbol{Q}$ are the F mass-scaled normal coordinates, where $F = 3N - 6$. $\hat{J}_\alpha$ and $\hat{\pi}_\alpha$ are the components of the total and vibrational angular momenta respectively, $\mu_{\alpha\beta}$ is the inverse of the effective moment of inertia, and $\alpha(\beta)$ represents the x, y, z coordinates. $V(\boldsymbol{Q})$ is the potential.

In many applications of this Hamiltonian in the literature, the vibrational angular momentum terms are neglected. We include these terms in MULTIMODE, and we have also performed some evaluations of neglecting them. For hydrogen atom motion, the errors can be on the order of 10 cm^{-1}.[38] An example where errors are larger is the ground-state tunneling splitting in H_3O^+.[60–62] Using the full Watson Hamiltonian, with an accurate PES, the calculated splitting is 52 cm^{-1},[62] close to the experimental value of 55 cm^{-1}. Without the vibrational angular momentum terms the calculated splitting is roughly 22 cm^{-1} lower.[61] This extreme example notwithstanding, neglect of these terms for larger molecules, e.g., ethylene glycol produces errors of the order of a wavenumber or less.[63]

III. VIBRATIONAL CONFIGURATION INTERACTION (VCI)

For a given Hamiltonian $\hat{H}$, the exact eigenfunctions, Ψ_L, can be written as

$$\Psi_L = \sum_K c_K^{(L)} \Phi_K, \tag{2}$$

where Φ_K are a complete, orthonormal set of functions. For example, these are the eigenfunctions of a zero-order, separable Hamiltonian. In this general case these are a direct product of functions in each mode. The goal is to obtain the expansion coefficients $c_K^{(L)}$. Once these are known, the problem is solved; however, the challenge remains to extract information from these coefficients that can be used to interpret the answer. Obviously, if a single coefficient dominates, e.g., has a magnitude of say 0.9 or greater, the interpretation is essentially the one from the familiar normal mode analysis, and the experimental band should be simple to interpret. The challenge comes from those interesting cases where there is not one or even several dominant coefficients. In such cases, one could conclude that the harmonic normal mode analysis has broken down and that there is strong mode-mode coupling. This is usually manifested experimentally by a broad and complex band, which is perforce difficult to interpret. The theoretical goal is then to determine at least which modes are strongly coupled and ultimately to understand the source of the coupling.

As an aside, we note that VPT2 theory approximates the expansion by

$$\Psi_K \approx \Phi_K + \sum_{L \neq K}^{\infty} \frac{\langle L|V'|K\rangle}{E_K^{(0)} - E_L^{(0)}} \Phi_L, \tag{3}$$

where $|L\rangle$ and $|K\rangle$ denote zero-order wavefunctions and $E_L^{(0)}$ and $E_K^{(0)}$ are the corresponding zero-order energies. As indicated, it is assumed that there is a dominant state Φ_K in this expansion. Typically these are from the separable harmonic approximation to the Watson Hamiltonian.

VCI methods ultimately lead to finding eigenvalues and eigenvectors of the matrix representation of $\hat{H}$, denoted $\boldsymbol{H}$. In MULTIMODE, the number of eigenvalues is user specified as this is a common parameter in matrix diagonalization routines. For the IR spectrum, the dipole moment must also be known and numerical quadrature is used in MULTIMODE to obtain the transition moments. As discussed next, the size of $\boldsymbol{H}$ is controlled by the excitation space and the dimensionality of the numerical quadratures for matrix elements; notably, those of the potential are controlled by the *n*-mode representation. There are numerous approaches to mitigate the size bottleneck of $\boldsymbol{H}$ and we refer the interested reader to the literature for details of some of these.[6,40] One effective approach is to use eigenfunctions of reduced-dimensionality Hamiltonians as the

basis.[6,64,65] A recent application of this approach, plus other effective methods to deal with potential matrix element evaluations, has been reported for vibrational energies of intermolecular modes of the water trimer using an accurate MLP.[66] Other recent and impressive calculations, using state-of-the-art variational methods, are for methanol,[67] the Eigen cation,[49] and the water dimer in full dimensionality.[68]

In the next section, we discuss specifically how MULTIMODE addresses the quadrature and H-matrix size bottleneck.

IV.   THE n-MODE REPRESENTATION OF POTENTIAL AND THE EXCITATION SPACE

MULTIMODE can use a force field as an input option, however, in general it makes use of MLPs, and matrix elements of the potential are done using multidimensional quadrature. Using straightforward direct-product, numerical quadrature scales exponentially with dimensionality. For example, if there are 10 quadrature points per degree of freedom, the quadrature space scales as $\mathcal{O}(10^F)$. Carrington and co-workers introduced a non-direct project quadrature method that mitigates this significantly[6,69]; however, even this method struggles for molecules with more than seven atoms.

In order to deal with this bottleneck the n-mode representation (nMR) of the potential was introduced by[23]

$$
\begin{aligned}
V(Q_1,\cdots,Q_F) = &\sum_i V_i^{(1)}(Q_i) + \sum_{i,j} V_{ij}^{(2)}(Q_i,Q_j) + \\
&\sum_{i,j,k} V_{ijk}^{(3)}(Q_i,Q_j,Q_k) + \\
&\sum_{i,j,k,l} V_{ijkl}^{(4)}(Q_i,Q_j,Q_k,Q_l) + \cdots,
\end{aligned}
\tag{4}
$$

where $V_i^{(1)}(Q_i)$ is the one-mode potential, i.e., the 1D cut through the full-dimensional PES in each mode, one-by-one, $V_{ij}^{(2)}(Q_i,Q_j)$ is the intrinsic 2-mode potential among all pairs of modes, etc. Here, intrinsic means that any n-mode term is zero if any of the arguments is zero. Also, each term in the representation is in principle of infinite order in the sense of a Taylor series expansion. For this representation to be useful it has to be truncated without significant loss of accuracy. After many applications, it has been established that truncation at the 4-mode term yields vibrational energies that differ from those truncated at the 3-mode term by at most 5–10 cm^{-1}. Tests can of

course be done by truncating at 5-mode terms. In MULTIMODE the maximum value of n is 6.

Numerical quadrature using this representation leads to a major reduction in the size of the quadrature space. For example truncating at 4-mode terms leads to a 4d quadrature space instead of a 24d quadrature space for the formic acid dimer. Also, we note that the nMR of the potential results in limitations on the size and dimensionality of the excitation space, for details see refs. 38,40.

Each term in the nMR of the potential can be obtained directly at quadrature points, for example as is done in MOLPRO.[46] Another option is to use interpolation to obtain these terms. This is an option in MULTIMODE using polynomial interpolation. Gaussian process regression has also been shown to be an effective approach.[70] This direct calculation of the terms allows for multi-scale and term-selection approaches.[71] However, for this paper which focuses on MLPs, we note that given an MLP it is straightforward and fast to obtain the nMR of it. In the applications below, as with virtually all our applications with MULTIMODE, an MLP is used. For larger molecules and especially molecular complexes where a full-dimensional MLP may not be necessary, a reduced dimensionality approach for the MLP is certainly possible. This was demonstrated nicely for the trimethyl-H_2O and trimethyl-CH_3OH complexes, where the trimethyl group is held fixed at its equilibrium structure.[72]

We close this section with remarks about the n-mode representation. Subsequent to the general nMR introduced in 1997,[23] the general "High Dimensional Model Representation" of the potential was introduced by Rabitz and co-workers.[73] The "cut" version of the representation is essential the nMR. Also, we note that the 2MR was introduced by Jung and Gerber[74] in 1996 and used extensively by the Gerber group. This is a very efficient, minimalist representation. However as shown in the literature, it does not produce results that are well-converged.[2,38] In general, this level of mode coupling cannot describe strong coupling among three or higher modes. Finally, we note that this representation has been used in VSCF/VCI calculations with other Hamiltonians, for example the general Podolsky Hamiltonian.[75]

Next, we demonstrate the success achieved using MULTIMODE with MLPs for two examples which feature diffuse IR bands.

V. TWO CHALLENGING CASE STUDIES

A. Formic Acid dimer

This is a ten-atom dimer bound by double hydrogen bonds, with a double-well barrier height of roughly 2850 cm^{-1} (8.2 kcal/mol).[76] It has been intensively studied experimentally[77–83] and theoretically.[76,84–99] Here the focus is on high-level MLPs that have been reported for this dimer[76,97–99] and quantum vibrational calculations using two of them. One of these PESs, denoted PIP,[76] is based on permutationally invariant polynomial regression,[100] and the second one HDNNP[98], is based on atom-centered high dimensional neural network regression.[101] Both are precise fits to thousands of CCSD(T) energies. The third MLP is a fit to thousands of MP2 energies and then transferred learned using a relatively small number of CCSD(T) energies. This PES is denoted PhyNet$_{TL}$[97] and is based on the atom centered neural network approach including properties such as forces and dipole moments.[102] First, we note that VPT2 calculations were reported using the more recent PhyNet$_{TL}$ and HDNNP PESs. These are overall in good agreement with each other and with experiment, except for the diffuse band spanning the CH and OH-stretch fundamentals. The PIP and HDNNP MLPs were used in reduced dimensionality VCI calculations.[98] Results of those calculations and comparison with experiment[98] are given in Table I below. Omitting discussion of the assignments, we simply note that the two MLPs (using very different regression architectures and different training datasets) give very similar energies. Agreement with experiment, albeit for the limited energy range available to these VCI calculations, is also very good.

Prior to these VCI calculations, we reported MULTIMODE VSCF/VCI calculations of the IR spectrum up to 3500 cm^{-1}, using 15-mode[103] and later 21 and full 24-mode calculations, with a 4MR of the PIP potential and a 3MR of the dipole moment surface.[104] Here we just show the diffuse band in the region of the CH- and OH-stretch fundamental, mentioned above. These results are shown in Figure 1. As seen, the VSCF/VCI calculations do capture the diffuse experimental band, albeit with some differences in the fine-structure seen in the experiment. The 24-mode VSCF/VCI band is less structured than the 21-mode one, although the two bands are certainly similar and agree in bread and overall intensity with experiment. For detailed discussions of this band the interested reader is referred to refs. 103–105. Finally, we note that VPT2 calculations using the HDNN PES predict sharp lines at 2920 and 2948 cm^{-1} in the region of this diffuse band.

9

TABLE I. VCI and experimental energies cm^{-1} for FAD given in ref. 98 for two machine-learned potentials described in the text.

Assignment	PIP[a]	HDNNP[b]	Exp
ν_{16}	70	70	69
$2\nu_{16}$	141	140	139
ν_{15}	162	171	168
ν_5/ν_8	191	190	161
ν_9/ν_9	208	210	194
$3\nu_{16}$	211	210	
$\nu_{15}+\nu_{16}$	232	240	
ν_{13}	239	243	242
ν_{24}	253	253	264
$\nu_9+\nu_{16}$	262	262	
$\nu_5+\nu_{16}$	277	279	
$4\nu_{16}$	281	280	
$\nu_{15}+2\nu_{16}$	303	309	
$\nu_{13}+\nu_{16}$	310	313	311
$\nu_{24}+\nu_{16}$	323	322	
$2\nu_{15}$	324	330	336
$\nu_5+2\nu_{16}$	332	337	
$\nu_8+2\nu_{16}$	347	348	

[a] Ref. 76

[b] Ref. 98

B. Protonated Oxalate Anion

The IR spectrum of the protonated oxalate anion $HO_2CCO_2^-$ is the second challenging case study. A diffuse band was reported in the OH-stretch region of IR spectrum in a 2015 joint experimental theoretical study.[106] This weak, broad band in the range 2500–3000 cm^{-1} attracted the attention of the theorists of that paper and those of subsequent theoretical studies.[57,107,108] Neither VPT2 nor classical or semi-quantum MD simulations were able to reproduce this band.
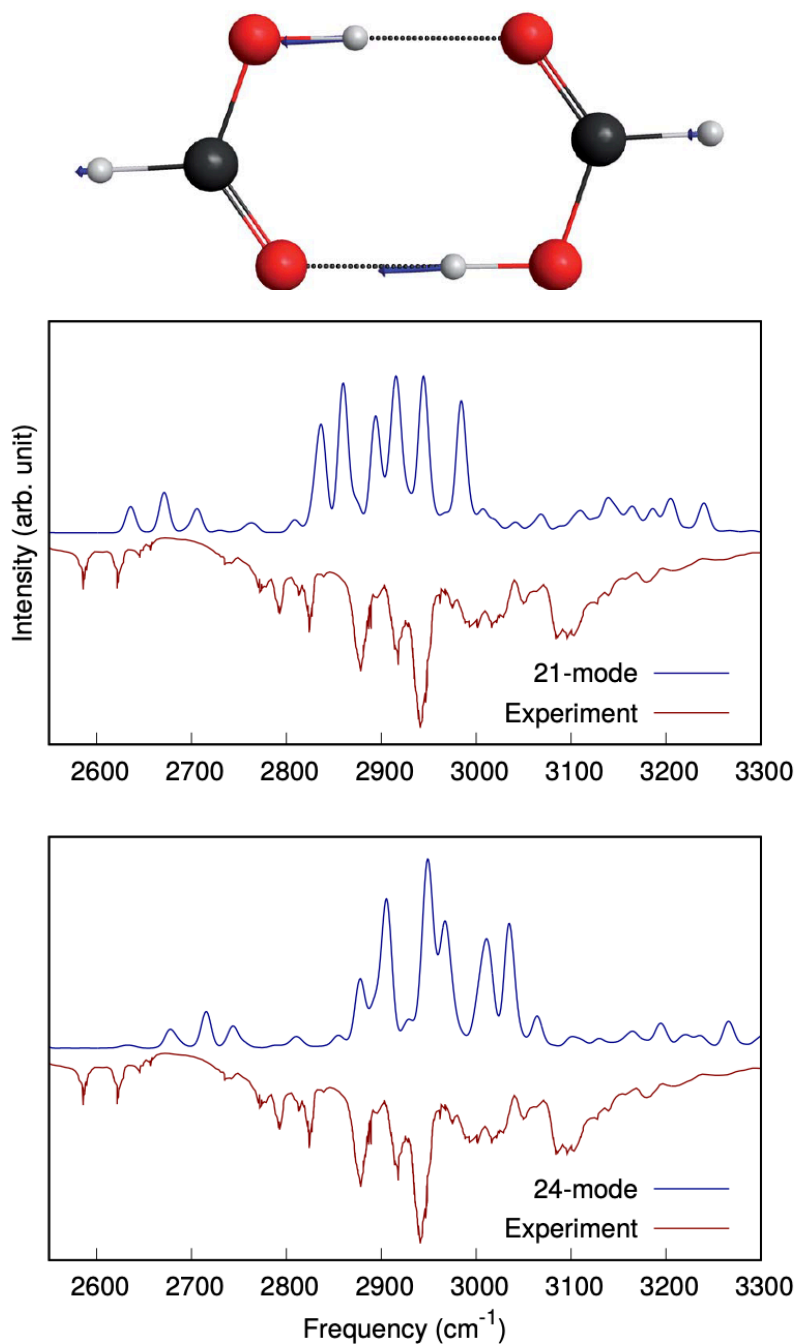
FIG. 1. Comparison of VSCF/VCI and experimental IR spectra including the diffuse OH-stretch for the formic acid dimer. Harmonic normal-mode eigenvector shown; harmonic frequency is 3325 cm^{-1}.

Stimulated by the experiments. we performed VSCF/VCI calculations of the IR spectrum using MULTIMODE and the PIP fits.[109] The MULTIMODE calculations were done in full dimensionality (15 modes) and for the spectra shown below the two-symmetry blocks of the H-matrix were

36,674 and 26,408 functions for symmetry block A' and A", respectively.

The comparisons with experiment for the normal and deuterated isotopolog are shown in Figure 2. As seen, the full spectra for protonated and deuterated cases agree well with experiment, and the highlight is the reproduction of the very diffuse bands, although fine-grained quantitative agreement is lacking. Detailed analyses of these bands as well as one for the tritiated isotopolog have been given elsewhere[109] and so we omit those here.
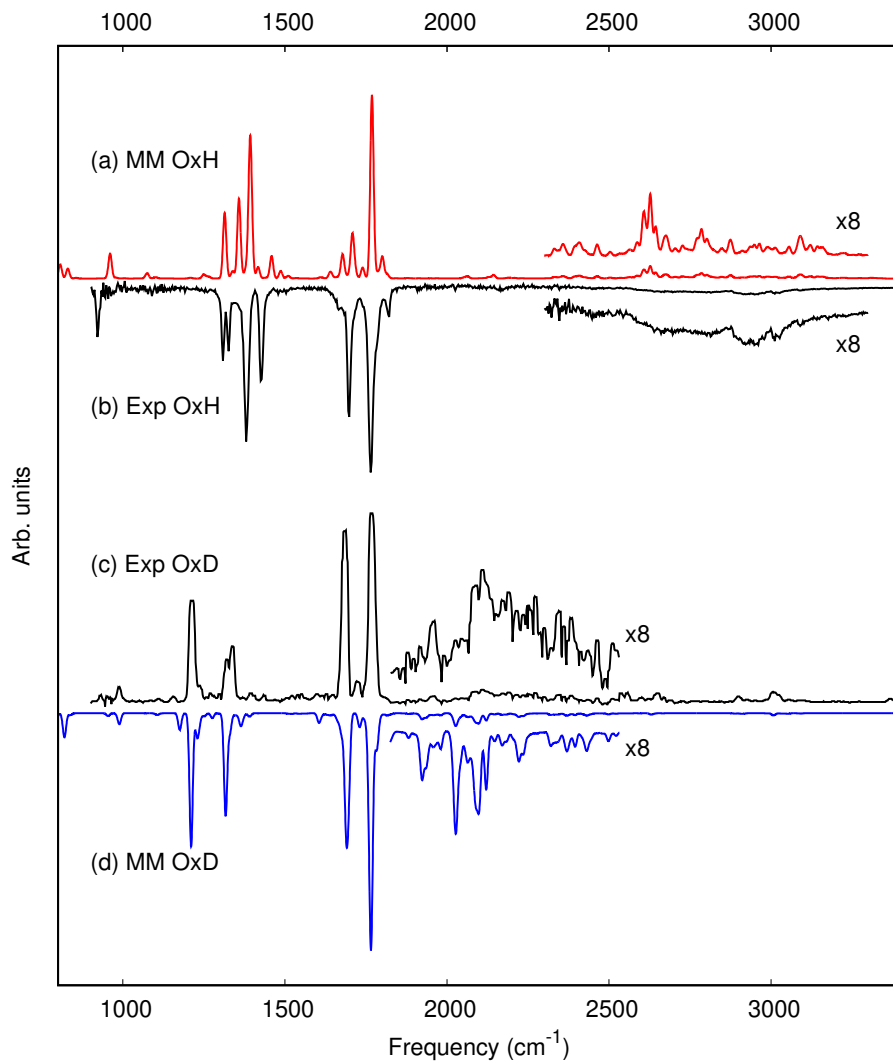

FIG. 2. IR spectra of $C_2O_4H^-$ (OxH) and $C_2O_4D^-$ (OxD) calculated using MULTIMODE VSCF/VCI

These two examples illustrate the power of the VSCF/VCI method, as implemented in MULTI-MODE and using accurate MLPs for challenging IR diffuse, fractionated bands. The calculations for these examples took less than 48 hours of cpu time. These highly fractionated bands cannot be described by VPT2, which assumes a dominant zero-order state. Such bands also present chal-

lenges for the VCI, VCC, and MCTDH software mentioned in the Introduction, both because of the number of atoms and the very strong coupling. That MULTIMODE succeeds in describing these bands illustrates a major strength of the normal-coordinate Watson Hamiltonian that is hard-coded into MULTIMODE. This Hamiltonian and coordinates describes stretch and stiff bending modes effectively. And often it is the fundamental excitation of these high-frequency modes, i.e., the stretches, that exhibit fractionation. This is because there are lower frequency modes that can be in low-order resonance with the higher-frequency fundamentals. Also, the density of states is greater at the energies of the stretch fundamentals than at the energy of the fundamentals of much lower-frequency modes. These facts fit nicely with the strengths of the MULTIMODE software.

There are weaknesses with these coordinates and the MULTIMODE software. Namely, very floppy motion such as methyl rotors or facile isomerization among low-lying conformers is not accurately described. Such motion is better described by curvilinear-coordinate approaches. However, the number of atoms, 10 for FAD and 7 for the protonated oxalate anion, present major computational challenges for such approaches, at present.

In the next section we describe two new software interfaces to MULTIMODE. One is a GUI to create the input and the second is an interface to enables MULTIMODE (written in Fortran) to call MLPs written in Python.

VI. NEW USER-FACING SOFTWARE FOR MULTIMODE

A. A GUI to create the input to MULTIMODE

MULTIMODE source code, documentation, including a Quickstart guide, two sample runs for H_2CO and the GUI described next are available at `https://github.com/szquchen/MULTIMODE`.

The single input file, fort.1, contains numerous options for running MULTIMODE, as described in the guides. In order to simplify creating this file, we have written a Python-based GUI to make an initial fort.1 file. The current usage is restricted to energies and eigenfunctions of non-linear molecules and with using normal-mode coordinates of a minimum. The user can select all $3N - 6$ normal modes or a subset of modes for the VSCF/VCI calculation. These modes are ordered 1 to $3N - 6$ in terms of increasing harmonic frequency. So mode 1 is the mode of lowest frequency. If a subset is used this set always includes the highest frequency and then keeps modes in order of decreasing frequency and drops the lowest frequency mode(s).

FIG. 3. Snapshot of the GUI to create the fort.1 input to MULTIMODE

A snapshot of the GUI is shown in Figure 3 for the example of H_2CO. Running this produces the input fort.1 file. Also, the meaning of the keywords is accessible via a click on them. More details about these parameters are given in the Quick Start guide in the Supplementary Material (SM).

This GUI is written in Python and is named "mmhelper.py" in the Github download.

B. PyFort

The potential (and other project-specific information) is called in the Fortran code "user.NAME.f", where "NAME" identifies the molecule or cluster. The call to the potential is SUBROUTINE GET-POT(V,NATOM,XX,RR), where the input is NATOM (the number of atoms) and XX, the array of Cartesian coordinates, which conforms to the order of the atoms read in fort.1. RR is an array of all bond lengths calculated in GETPOT and V is the potential in atomic units. This can be a totally general form including MLPs. For the formic acid dimer and protonated oxalate examples, these potentials are PIPs MLPs, which are in written Fortran 90 and which are directly called in GETPOT.

Previously, MULTIMODE, which as noted already is written and so the MLPs were also required to be written in Fortran. Currently many MLPs are written in Python, owing to the availability of powerful ML software, e.g., Neural Network regression, written in Python. So it would be desirable to develop software that enables MULTIMODE to communicate with Python. This is now a general issue in Computational Chemistry where so much legacy codes is written in Fortran.

We have developed such interface software, which we term "PyFort". Fortran and Python are joined together using this interface code through a C wrapper. The Fortran code uses the ISO C binding feature to interface with the C code, and the C code is bound to the Python code. A schematic flow diagram of this software is given in Figure 4. Since MULTIMODE requires at a minimum potential energies, we have implemented this functionality in the current interface. (The interface is general and so it can be used for forces, etc., if available.) Although there are several ways to implement the interface described above, we chose to explicitly write the interface codes for portability performance reasons. The interface codes in Fortran, C, and Python are given in the SM, along with a brief discussion of some of the details of the implementation, for two example MLPs described below.

As one demonstration we use the PhysNet oxalate potential mentioned above. This code requires construction of the neural network layers and initialization of the weights. This step is relatively expensive, but is required only once, so our interface code includes an initialization function to start the Python interpreter and perform this step. The Python interpreter and the oxalate potential neural network persist for the entirety of the MULTIMODE calculations. The oxalate potential is called many times during the MULTIMODE calculation. At the termination of the MULTIMODE run, a finalization routine is called to halt the Python interpreter. In this

GETPOT (Fortran)

Module pes_interface (Fortran)
iso_c_binding

C wrapper
call python function

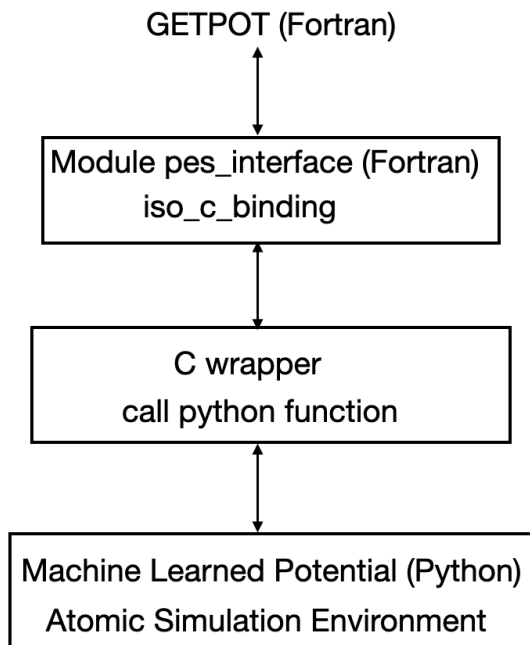Machine Learned Potential (Python)
Atomic Simulation Environment

FIG. 4. Schematic Flow Diagram for PyFort Interface

manner, we achieve a performant interface to the oxalate potential energy surface code enabling its use with MULTIMODE.

VSCF/VCI vibrational energies, using an efficient 2MR of the PhysNet MLP are shown in Figure 5 along with corresponding ones using the PIP MLP as a standard correlation plot. As seen, there is excellent agreement for the two PESs. This is not unexpected as both PESs are precise fits to the same datasets.[57]

A second example is the "universal" force field MACE-OFF.[58] This has been interfaced to MULTIMODE, using PyFort and successfully tested for formaldehyde, H_2CO. The details of the interface software are given in the SM.

To conclude this subsection, we note that PyFort is general and could be used for many other applications. For example, software for computational spectroscopy using semi- or quasi-classical methods is often written in Fortran.[110,111] (Note, a free web-platform to calculate vibrational spectra from a quasi-classical trajectory molecular dynamics adopts python software to compute the spectrum and a web interface to facilitate user interaction and software execution.[112,113])
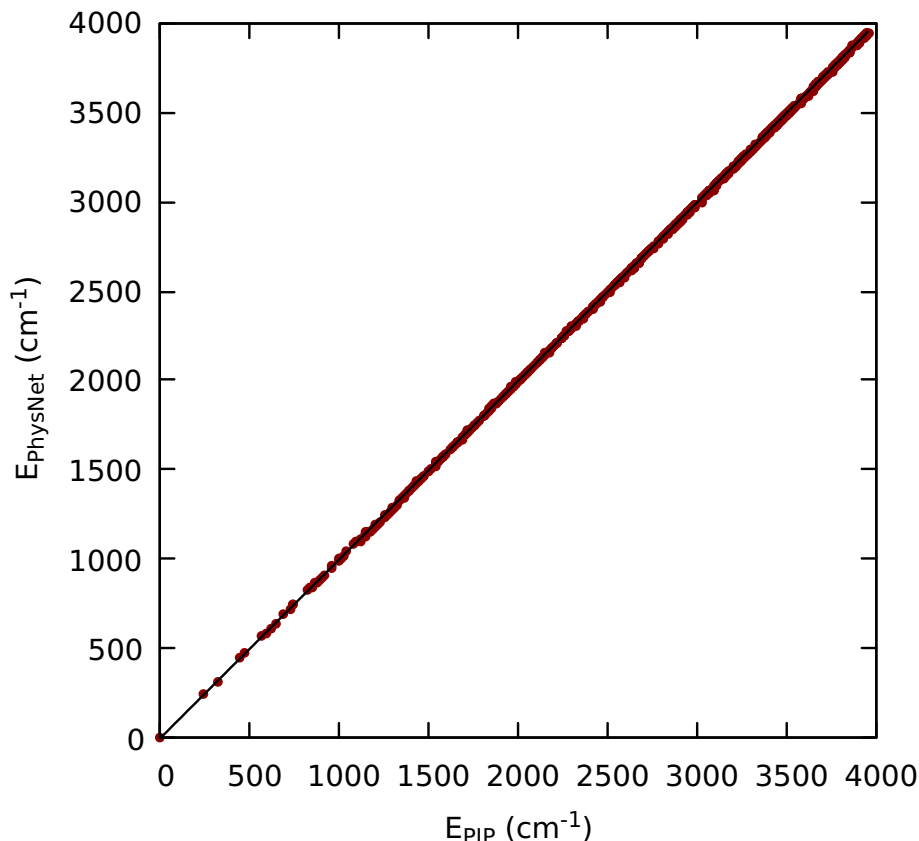
16

FIG. 5. Correlation plot of the first 600 eigenenergies from MULTIMODE calculations on protonated oxalate using PIP PES and PhysNet PES. The root mean square difference between the two MLP energies is $6\,\mathrm{cm}^{-1}$.

VII. SUMMARY AND CONCLUSIONS

The vibrational dynamics and spectroscopy of molecules and molecular clusters continues to be an active research area both experimentally and theoretically. The computational software MUL-TIMODE that performs VSCF/VCI calculations was briefly described along with two challenging applications to the formic acid dimer and the protonated oxalate anion. Two user-friendly software interfaces were introduced for MULTIMODE with the options shown in Figure 6. One is an interactive GUI that facilitates the creation of the input file. The second, PyFort, is an interface that enables MULTIMODE, written in Fortran, to call machine-learned potentials written in Python. Two examples of the usage were given, one for the PhysNet potential for protonated oxalate anion and the second for MACE-OFF.

17

<div style="border: 2px solid green; padding: 1em;">

MULTIMODE Highlights and New Features

- Eigenvalues and eigenfunctions of the Watson Hamiltonian
- VSCF and VSCF/VCI
- n-mode representation of the potential
- General user-supplied potential
- Option to reduce number modes to couple
- Vibrational spectra J = 0
- Expectation values
- GUI for input and MULTIMODE and Documentation at
  https://github.com/szquchen/MULTIMODE/tree/main
- Interface "PyFort" to call Python potentials

</div>

FIG. 6. Outline of selected and new features of MULTIMODE

SUPPLEMENTARY MATERIAL

Details of the PyFort Interface to the PhysNet Oxalate Potential Energy Surface and MACE-OFF "universal" force field written in Python and the one-page Quick Start guide.

ACKNOWLEDGMENTS

DATA AVAILABILITY STATEMENT

The data that supports the findings of this study are available within the article and its supplementary material. The MULTIMODE program is available at `https://github.com/szquchen/MULTIMODE`.

REFERENCES

[1] J. M. Bowman, ed., *Vibrational Dynamics of Molecules* (World Scientific, 2022).

[2]J. M. Bowman, T. Carrington, and H.-D. Meyer, Mol. Phys. **106**, 2145 (2008).

[3]M. Hochlaf, Phys. Chem. Chem. Phys. **15**, 9967 (2013).

[4]M. L. Senent, M. Hochlaf, and M. Carvajal, J. Phys. Chem. A **120**, 475 (2016).

[5]J. Tennyson, J. Chem. Phys. **145**, 120901:1 (2016).

[6]T. Carrington, J. Chem. Phys. **146**, 120902:1 (2017).

[7]C. Qu and J. M. Bowman, Phys. Chem. Chem. Phys. **21**, 3397 (2019).

[8]H. H. Nielsen, Rev. Mod. Phys. **23**, 90 (1951).

[9]J. F. Gaw, A. Willetts, W. H. Green, and N. C. Handy, in *Advances in Molecular Vibrations and Collision Dynamics*, edited by J. M. Bowman and M. A. Ratner (1991) p. 169.

[10]V. Barone, J. Bloino, C. A. Guido, and F. Lipparini, Chem. Phys. Lett. **496**, 157 (2010).

[11]J. Bloino and V. Barone, J. Chem. Phys. **136**, 124108:1 (2012).

[12]D. Mitoli, A. Erba, V. Barone, and M. Mendolicchio, J. Phys. Chem. Lett. **16**, 9956 (2025).

[13]Q. Yu, J. M. Bowman, R. C. Fortenberry, J. S. Mancini, T. J. Lee, T. D. Crawford, W. Klemperer, and J. S. Francisco, J. Phys. Chem. A **119**, 11623 (2015).

[14]D. A. Matthews, J. Vázquez, and J. F. Stanton, Mol. Phys. **105**, 2659 (2007).

[15]M. E. Kellman, The Journal of Chemical Physics **93**, 6630 (1990).

[16]I. Sibert, Edwin L., The Journal of Chemical Physics **88**, 4378 (1988).

[17]A. B. McCoy and E. L. S. III, Mol. Phys. **77**, 697 (1992).

[18]K. Yagi and H. Otaki, J. Chem. Phys. **140**, 084113 (2014).

[19]K. Yagi and B. Thomsen, J. Phys. Chem. A **121**, 2386 (2017).

[20]J. M. Bowman, J. Chem. Phys. **68**, 608 (1978).

[21]G. D. Carney, L. L. Sprandel, and C. W. Kern, Adv. Chem. Phys. **37**, 305 (1978).

[22]J. M. Bowman, Acc. Chem. Res. **19**, 202 (1986).

[23]S. Carter, S. J. Culik, and J. M. Bowman, J. Chem. Phys. **107**, 10458 (1997).

[24]R. B. Gerber and M. A. Ratner, Adv. Chem. Phys. , 97 (1998).

[25]T. K. Roy and R. B. Gerber, Phys. Chem. Chem. Phys. **15**, 9468 (2013).

[26]A. Erba, J. Maul, M. Ferrabone, R. Dovesi, M. Rérat, and P. Carbonnière, J. Chem. Theory Comput. **15**, 3766 (2019).

[27]L. S. Norris, M. A. Ratner, A. E. Roitberg, and R. B. Gerber, J. Chem. Phys. **105**, 11261 (1996).

[28]L. Pele and R. B. Gerber, The Journal of Chemical Physics **128**, 165105 (2008).

[29]K. Christoffel and J. Bowman, Chem. Phys. Lett. **85**, 220 (1982).

[30]O. Christiansen, Phys. Chem. Chem. Phys. **14**, 6672 (2012).

[31] R. B. Jensen and O. Christiansen, J. Chem. Phys. **162**, 084112 (2025).

[32] R. Whitehead and N. Handy, J. Molec. Spectro. **55**, 356 (1975).

[33] G. Avila and T. Carrington, J. Chem. Phys. **147**, 144102 (2017).

[34] B. Schröder, G. Rauhut, and J. Bowman, *Vibrational configuration interaction theory* (World Scientific Singapore, 2022).

[35] A. U. Bhatty and K. R. Brorsen, Molec. Phys. **119**, e1936250 (2021).

[36] H. K. Tran and T. C. Berkelbach, J. Chem. Phys. **159**, 194101 (2023).

[37] J. H. Fetherolf and T. C. Berkelbach, J. Chem. Phys. **154**, 074104 (2021).

[38] J. M. Bowman, S. Carter, and X. Huang, Int. Rev. Phys. Chem. **22**, 533 (2003).

[39] S. Carter, J. M. Bowman, and N. C. Handy, Theor. Chem. Acc. **100**, 191 (1998).

[40] Q. Yu, C. Qu, P. L. Houston, R. Conte, A. Nandi, and J. M. Bowman, in *Vibrational Dynamics of Molecules*, edited by J. M. Bowman (World Scientific, 2022).

[41] E. Matyus, G. Czakó, and A. G. Császár, J. Chem. Phys. **130**, 134112 (2009).

[42] A. G. Császár, C. Fabri, T. Szidarovszky, E. Matyus, T. Furtenbacher, and G. Czakó, Phys. Chem. Chem. Phys. **14**, 1085 (2012).

[43] S. N. Yurchenko, W. Thiel, and P. Jensen, J. Molec. Spectros. **245**, 126 (2007).

[44] W. Mizukami and D. P. Tew, The Journal of Chemical Physics **139**, 194108 (2013).

[45] M. Sibaev and D. L. Crittenden, Computer Physics Communications **203**, 290 (2016).

[46] H.-J. Werner, P. J. Knowles, F. R. Manby, J. A. Black, K. Doll, A. Heßelmann, D. Kats, A. Köhn, T. Korona, D. A. Kreplin, Q. Ma, T. F. Miller, A. Mitrushchenkov, K. A. Peterson, I. Polyak, G. Rauhut, and M. Sibaev, J. Chem. Phys. **152**, 144107:1 (2020).

[47] O. Christiansen, D. Artiukhin, F. Bader, I. Godtliebsen, E. Gras, W. Györffy, M. Hansen, M. Hansen, M. Højlund, N. Høyer, *et al.*, "Midascpp 2025.10.0," `https://midascpp.gitlab.io/index.html` (2025), accessed: 2025-10.

[48] N. Glaser, A. Baiardi, and M. Reiher, Vibrational Dynamics of Molecules , 80 (2022).

[49] M. Rano and H. R. Larsson, J. Chem. Phys. **163**, 164110 (2025).

[50] H.-D. Meyer, U. Manthe, and L. S. Cederbaum, Chem. Phys. Lett. **165**, 73 (1990).

[51] H. Meyer, M. Schröder, and O. Vendrell, Vibrational Dynamics Of Molecules , 340 (2022).

[52] D. Bégué, N. Gohaud, C. Pouchan, P. Cassam-Chenaï, and J. Liévin, J. Chem. Phys. **127**, 164115 (2007).

[53] S. Erfort, M. Tschöpe, and G. Rauhut, J. Chem. Phys. **152**, 244104:1 (2020).

[54] Q. Yu, C. Qu, P. Houston, R. Conte, A. Nandi, and J. M. Bowman, Vibrational Dynamics Of Molecules , 296 (2022).

[55] S. Carter, A. R. Sharma, J. M. Bowman, P. Rosmus, and R. Tarroni, J. Chem. Phys. **131**, 224106 (2009).

[56] S. Carter, A. R. Sharma, and J. M. Bowman, J. Chem. Phys. **137**, 154301 (2012).

[57] V. Andreichev, S. Käser, E. L. Bocanegra, M. Salik, M. A. Johnson, and M. Meuwly, Physical Chemistry Chemical Physics **27**, 23288 (2025).

[58] D. P. Kovács, J. H. Moore, N. J. Browning, I. Batatia, J. T. Horton, Y. Pu, V. Kapil, W. C. Witt, I.-B. Magdău, D. J. Cole, and G. Csányi, J. Am. Chem. Soc. **147**, 17598 (2025).

[59] J. K. G. Watson, Mol. Phys. **15**, 479 (1968).

[60] X. Huang, S. Carter, and J. Bowman, J. Chem. Phys. **118**, 5431 (2003).

[61] E. Kamarchik, Y. Wang, and J. Bowman, J. Phys. Chem. A **113**, 7556 (2009).

[62] Q. Yu and J. M. Bowman, J. Chem. Theory Comput. **12**, 5284 (2016).

[63] A. Nandi, R. Conte, P. Pandey, P. L. Houston, C. Qu, Q. Yu, and J. M. Bowman, J. Chem. Theory Comput. **21**, 5208 (2025).

[64] J. M. Bowman and B. Gazdy, J. Chem. Phys. **94**, 454 (1991).

[65] S. Zou, J. M. Bowman, and A. Brown, J. Chem. Phys. **118**, 10012 (2003).

[66] I. Simkó, P. M. Felker, and Z. Bačić, J. Chem. Phys. **162**, 034301 (2025).

[67] A. Sunaga, T. Győri, G. Czakó, and E. Mátyus, J. Chem. Phys. **163**, 064101 (2025).

[68] X.-G. Wang, S. Yang, J. Carrington, Tucker, and D. H. Zhang, J. Chem. Phys. **163**, 144308 (2025).

[69] G. Avila and T. Carrington, J. Chem. Phys. **143**, 214108 (2015).

[70] G. Schmitz, D. G. Artiukhin, and O. Christiansen, J. Chem. Phys. **150**, 131102:1 (2019).

[71] D. G. Artiukhin, E. L. Klinting, C. König, and O. Christiansen, J. Chem. Phys. **152**, 194105 (2020).

[72] S. Jiang, M. Su, S. Yang, C. Wang, Q.-R. Huang, G. Li, H. Xie, J. Yang, G. Wu, W. Zhang, Z. Zhang, J.-L. Kuo, Z.-F. Liu, D. H. Zhang, X. Yang, and L. Jiang, J. Phys. Chem. Lett. **12**, 2259 (2021).

[73] H. Rabitz and Ö. F. Ali§, J. Math. Chem. **25**, 197 (1999).

[74] J. O. Jung and R. B. Gerber, J. Chem. Phys. **105**, 10332 (1996).

[75] M. Schneider and G. Rauhut, J. Chem. Phys. **160**, 214118 (2024).

[76] C. Qu and J. M. Bowman, Phys. Chem. Chem. Phys. **18**, 24835 (2016).

[77] F. Ito and T. Nakanaga, Chem. Phys. **277**, 163 (2002).

[78] Ö. Birer and M. Havenith, Annu. Rev. Phys. Chem. **60**, 263 (2009).

[79] K. G. Goroya, Y. Zhu, P. Sun, and C. Duan, J. Chem. Phys. **140**, 164311 (2014).

[80] D. Luckhaus, J. Phys. Chem. A **110**, 3151 (2006).

[81] F. Ito, Chem. Phys. Lett. **447**, 202 (2007).

[82] D. Luckhaus, Phys. Chem. Chem. Phys. **12**, 8357 (2010).

[83] Y. H. Yoon, M. L. Hause, A. S. Case, and F. F. Crim, J. Chem. Phys. **128**, 084305 (2008).

[84] M. V. Vener, S. Scheiner, and N. D. Sokolov, J. Chem. Phys. **101**, 9755 (1994).

[85] S. Miura, M. E. Tuckerman, and M. L. Klein, J. Chem. Phys. **109**, 5290 (1998).

[86] M. V. Vener, O. Kühn, and J. M. Bowman, Chem. Phys. Lett. **349**, 562 (2001).

[87] P. R. L. Markwick, N. L. Doltsinis, and D. Marx, J. Chem. Phys. **122**, 054112 (2005).

[88] W. Siebrand, Z. Smedarchina, and A. Fernández-Ramos, Chem. Phys. Lett. **459**, 22 (2008).

[89] G. L. Barnes, S. M. Squires, and E. L. Sibert, J. Phys. Chem. B **112**, 595 (2008).

[90] I. Matanović, N. Došlić, and B. R. Johnson, J. Chem. Phys. **128**, 084103 (2008).

[91] G. V. Mil'nikov, O. Kühn, and H. Nakamura, J. Chem. Phys. **123**, 074308 (2005).

[92] A. Jain and E. L. Sibert, J. Chem. Phys. **142**, 084115 (2015).

[93] S. D. Ivanov, I. M. Grant, and D. Marx, J. Chem. Phys. **143**, 124304 (2015).

[94] G. A. Pitsevich, A. E. Malevich, E. N. Kozlovskaya, I. Y. Doroshenko, V. Sablinskas, V. Pogorelov, D. Dovgal, and V. Balevicius, Vib. Spectrosc. **79**, 67 (2015).

[95] K. Mackeprang, Z. H. Xu, Z. Maroun, M. Meuwly, and H. G. Kjaergaard, Phys. Chem. Chem. Phys. **18**, 24654 (2016).

[96] J. O. Richardson, Phys. Chem. Chem. Phys. **19**, 966 (2017).

[97] S. Käser and M. Meuwly, Physical Chemistry Chemical Physics **24**, 5269 (2022).

[98] D. Shanavas Rasheeda, A. Martín Santa Daría, B. Schröder, E. Mátyus, and J. Behler, Phys. Chem. Chem. Phys. **24**, 29381 (2022).

[99] F. Li, X. Yang, X. Liu, J. Cao, and W. Bian, ACS Omega **8**, 17296 (2023).

[100] B. J. Braams and J. M. Bowman, Int. Rev. Phys. Chem. **28**, 577 (2009).

[101] J. Behler, J. Chem. Phys. **134**, 074106 (2011).

[102] O. T. Unke and M. Meuwly, J. Chem. Theory Comput. **15**, 3678 (2019).

[103] C. Qu and J. M. Bowman, J. Chem. Phys. **148**, 241713 (2018).

[104] C. Qu and J. M. Bowman, Faraday Discuss. **212**, 33 (2018).

[105] P. Houston, B. L. Van Hoozen, C. Qu, Q. Yu, and J. M. Bowman, Faraday Discuss. **212**, 65 (2018).

[106] C. T. Wolke, A. F. DeBlase, C. M. Leavitt, A. B. McCoy, and M. A. Johnson, J. Phys. Chem. A **119**, 13018 (2015).

[107] Z.-H. Xu and M. Meuwly, J. Phys. Chem. A **121**, 5389 (2017).

[108] D. Boutwell, D. Pierre-Jacques, O. Cochran, J. Dyke, D. Salazar, C. Tyler, and M. Kaledin, J. Phys. Chem. A **126**, 583 (2022).

[109] C. Qu, P. L. Houston, and J. M. Bowman, J. Chem. Phys. **under review** (2026).

[110] M. Ceotto, G. Di Liberto, and R. Conte, Phys. Rev. Lett. **119**, 010401 (2017).

[111] R. Conte, G. Mandelli, G. Botti, D. Moscato, C. Lanzi, M. Cazzaniga, C. Aieta, and M. Ceotto, Chem. Sci. **16**, 20 (2025).

[112] M. Gandolfi, D. Moscato, C. Aieta, M. Pindaro, E. Campana, S. Valtolina, and M. Ceotto, "A web platform for time averaged fourier transform of autocorrelated data," (2024), accessed on Dec 16, 2025.

[113] R. Conte, M. Gandolfi, D. Moscato, C. Aieta, S. Valtolina, and M. Ceotto, J. Comput. Chem. **46**, e70118 (2025).